Atmospheric
Chemistry
and Physics

Exceptional emissions of NH_3 and HCOOH in the 2010 Russian wildfires

Y. R'Honi[1], **L. Clarisse**[1], **C. Clerbaux**[1,2], **D. Hurtmans**[1], **V. Duflot**[1], **S. Turquety**[3], **Y. Ngadi**[1], and **P.-F. Coheur**[1]

[1]Spectroscopie de l'Atmosphère, Chimie Quantique et Photophysique, Université Libre de Bruxelles (U.L.B.), Brussels, Belgium
[2]UPMC Univ. Paris 06, Université Versailles St.-Quentin, CNRS/INSU, LATMOS-IPSL, Paris, France
[3]UPMC Univ. Paris 06, CNRS/INSU, LMD-IPSL, Paris, France

Correspondence to: Y. R'Honi (yrhoni@ulb.ac.be)

Abstract. In July 2010, several hundred forest and peat fires broke out across central Russia during its hottest summer on record. Here, we analyze these wildfires using observations of the Infrared Atmospheric Sounding Interferometer (IASI). Carbon monoxide (CO), ammonia (NH_3) and formic acid (HCOOH) total columns are presented for the year 2010. Maximum total columns were found to be one order (for CO and HCOOH) and two orders (for NH_3) of magnitude larger than typical background values. The temporal evolution of NH_3 and HCOOH enhancement ratios relative to CO are presented. Evidence of secondary formation of HCOOH is found, with enhancement ratios exceeding reported emission ratios in fresh plumes. We estimate the total emitted masses for the period July–August 2010 over the center of western Russia; they are 19–33 Tg (CO), 0.7–2.6 Tg (NH_3) and 0.9–3.9 Tg (HCOOH). For NH_3 and HCOOH, these quantities are comparable to what is emitted in the course of a whole year by all extratropical forest fires.

1 Introduction

Biomass burning is a major source of atmospheric trace gases and aerosols (Crutzen and Andreae, 1990). Boreal forest fires contribute significantly to these emissions and are also important as they can severely affect air quality in populated regions of the Northern Hemisphere (Langmann et al. (2009) and references therein). Many laboratory, field and aircraft studies have been conducted to characterize the composition of fire plumes (Andreae and Merlet, 2001; Akagi et al.,

2011), but uncertainties remain due to the lack of measurements over larger areas or periods; this is particularly true for the total emission of reactive species.

The polar orbiting Infrared Atmospheric Sounding Interferometer (IASI), which measures globally the Earth's outgoing infrared radiation at a high spectral resolution and low instrumental noise (Clerbaux et al., 2009), is an excellent tool for observing and analyzing trace gas emissions from strong fire events (Coheur et al., 2009; Turquety et al., 2009; Clarisse et al., 2011). Its potential to monitor CO (carbon monoxide) from vegetation burning has frequently been used. Measurements of other fire emission products, such as NH_3 (ammonia) or volatile organic compounds, have in contrast not much been exploited. Such measurements can directly improve our knowledge of fire emissions and fluxes. These currently rely on the remote sensing of fire counts (e.g. Kasischke et al., 2003) and fire radiation power (e.g. Wooster et al., 2005), with application of tabulated average values of emission factors. Here we study simultaneous CO, NH_3 and HCOOH (formic acid) fire emissions in the 2010 Russian fires. It is the first time that such a large spatial- and temporal-scale case study for a fire event is undertaken for NH_3 and HCOOH. IASI CO observations of these fires (Yurganov et al., 2011; Krol et al., 2012) are used to test our methodology and for the calculation of enhancement ratios. We use total columns of NH_3 and CO from the FORLI (Fast-Optimal Estimation Retrievals on Layers for IASI) near-real-time retrieval software (Hurtmans et al., 2012) and a retrieval scheme based on brightness temperature difference between a perturbed and a reference channel (BTD) for HCOOH

(Razavi et al., 2011). Only the daytime data, which are more sensitive to surface concentrations, have been used. In addition, NH$_3$ and HCOOH are retrieved only when enough spectral information is available (see Sect. 5).

Formic acid is an important volatile organic compound in the atmosphere; but uncertainties in its global budget remain large (Stavrakou et al., 2011). The majority is photochemically produced from non-methane hydrocarbons. It is also released directly in the atmosphere from terrestrial vegetation and biomass burning, for which the total (primary) emissions account for 1–4 Tg yr^{-1} (Paulot et al., 2011; Stavrakou et al., 2011). NH$_3$ is the most important base in the atmosphere and is released primarily from agriculture (76 %), natural sources (19 %) and fossil fuel burning (5 %). Natural fires only account for 4 % of the total emissions totaling 5–15 Tg yr^{-1} (European Commission, Joint Research Centre (JRC)/Netherlands Environmental Assessment Agency (PBL), 2011).

During the summer of 2010, central European Russia endured the driest and hottest July ever recorded. Witte et al. (2011) reported anomalously high temperatures (35–41 °C, compared to average temperatures of 15–20 °C usually observed in the summer season) and low relative humidity (9–25 %) from mid-June to mid-August 2010, from radiosonde measurements in western Russia. The intense heat and drought wave initiated hundreds of wildfires in European Russia and burned forests, grasslands, croplands, fields and urbanized areas across a massive region around Moscow (Shvidenko et al., 2011), severely affecting the air quality (Elansky et al., 2011a,b; Fokeeva et al., 2011; Konovalov et al., 2011; Zvyaginstev et al., 2011; Golitsyn et al., 2012). The unusual magnitude of the event was revealed for instance by high values of the fire radiative power, which reached 19 000 MW close to Moscow (Witte et al., 2011); this is 400 times more than what is observed on average in Russia (Wooster and Zhang, 2004). Along this, large emissions of aerosols and trace gases such as CO, tropospheric nitrogen oxides (NO$_2$), ozone (O$_3$) and formaldehyde (HCHO) have been reported, using measurements from a variety of satellite sounders (Konovalov et al., 2011; Yurganov et al., 2011; Chubarova et al., 2012; Huijnen et al., 2012; Krol et al., 2012).

In the next section we present the CO, NH$_3$ and HCOOH total column maximums observed within a 2 month period (1 July to 1 September) in the summer of 2010, and the mean total columns for these species for the year 2010 over the area 40–75° N and 30–150° N. Section 3 presents the calculation and temporal evolution of the enhancement ratios of NH$_3$ and HCOOH relative to CO. In Sect. 4, we calculate the total masses and the extra burden due to fires, the fluxes in Tg day^{-1}, as well as the total emitted masses over the entire burning period. The issues of surface sensitivity, the related measurement uncertainties and how they affect the presented results are briefly discussed in Sect. 5. In Sect. 6 we summarize our findings, in particular on the magnitude of the exceptional HCOOH and NH$_3$ emissions.

2 Distributions and time series of total columns

Average total columns of CO, NH$_3$ and HCOOH are shown in Fig. 1 over Europe and Asia in grid cells of 0.5° × 0.5°, from 27 July (corresponding to the first IASI observation of the fire plumes) to 27 August (a few days after the end of the fires) of 2010. There are some differences between the spatial extents of CO, NH$_3$ and HCOOH. These can be explained by differences in lifetime (see Sect. 4), but also by the fact that we have a more limited sensitivity above 55° N for NH$_3$ and HCOOH related to thermal contrast (see Sect. 5). Note also that the red box in Fig. 1, extending in the area of 40–75° N and 30–150° N, is the same area as the one considered in the study of Yurganov et al. (2011). This choice was made intentionally to facilitate the comparison of our results to that earlier study.

Very high total columns were observed during the event for the three species. Figure 2a shows the temporal evolution of the retrieved total column maximums during a two month period that includes the fires (1 July to 1 September 2010) in the area corresponding to the red box in Fig. 1; Fig. 2b shows the mean total columns for the year 2010 covering the same area. In Fig. 2a one sees a significant increase of total columns at the end of July, which corresponds to the beginning of the fires (more precisely on 27 July) reaching a maximum emission on 2, 10 and 15 August respectively for CO, HCOOH and NH$_3$. For NH$_3$ the maximum columns have been observed close to the sources, at around 500 km southeast of Moscow. For CO and HCOOH these were observed somewhat further, at around 1000 km southeast of Moscow. These values are 40 times (for CO and HCOOH) and more than 300 times (for NH$_3$) higher than the typical background values which were calculated as the mean of the daily minimum columns measured with IASI before the fire period (from 1–26 July).

As the BTD retrieval method of HCOOH was not designed for such exceptional columns, we have performed independent optimal estimation retrievals (OEM) to verify these results. Since these are time consuming they were applied only over a small area (54–57° N and 47–54° N) and for a few days (from 27 July to 10 August 2010). The OEM retrievals yield total columns which are on average a factor two smaller than the BTDs retrievals (around 1.5 for columns higher than 5×10^{16} molec cm^{-2} and 2.3 for columns lower than 5×10^{16} molec cm^{-2}). The observed differences between the two retrieval approaches could point to limitations of the BTD retrieval method for this specific event. On the other hand also OEM retrievals are prone to errors (including the important smoothing errors when the sensitivity is low). The discrepancy clearly shows the difficulty in the measuring accurate concentrations for this species. As far as we know,
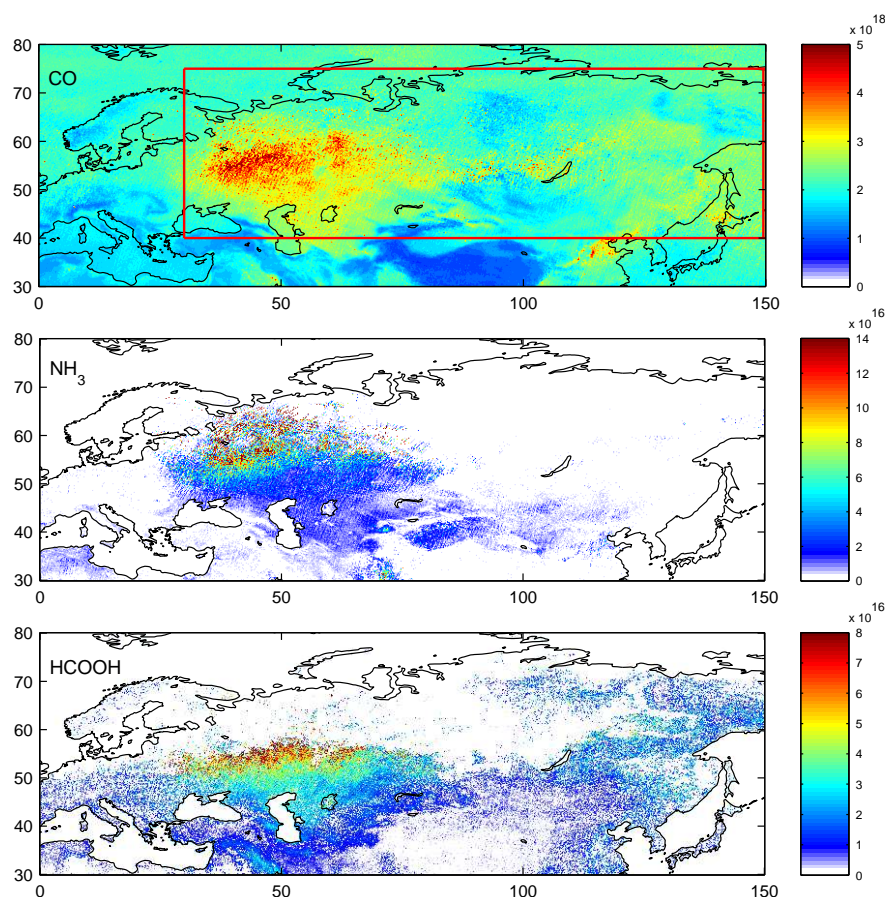
Fig. 1. IASI morning observations of the 2010 Russian wildfires plumes. The 3 panels show the mean CO, NH₃ and HCOOH total columns in molec cm^{-2}, in grid cells of $0.5° \times 0.5°$ for one month, from 27 July to 27 August 2010.

there have been no independent measurements of formic acid in the Russian fires, so that we cannot resolve this uncertainty at this stage. However, in what follows it is important to keep in mind that all HCOOH columns and derived quantities (enhancement ratios, total masses and fluxes) are possibly overestimated by a factor 1.5 to 2.3.

The maximum observed columns of both HCOOH and NH₃ quickly return to typical background values after August 20. This decrease is especially pronounced for NH₃, which is the shortest-lived species of the three. The mean CO total columns, presented here (Fig. 2b), are in good agreement with recent studies of Yurganov et al. (2011), Witte et al. (2011) and Mielonen et al. (2012), which reported mean values between 2 and 4×10^{18} molec cm^{-2} in different areas around Moscow. The higher than average CO total columns observed above central Russia between January and June 2010 (Fig. 2b) are due to the usual seasonality of that species, maybe intensified in springtime by the transport of fire plumes from outside the studied region (Parrington et al., 2012). Similarly, the progressive increase in NH₃ and HCOOH from March to the start of the fires can be explained

with the increase in spring of agricultural activities (for NH₃) (Clarisse et al., 2009) and plant growth (for HCOOH). The seasonality in HCOOH seen by IASI here is in a good agreement with those reported by Grutter et al. (2010) in the upper troposphere as observed by MIPAS (Michelson Interferometer for Passive Atmospheric Sounding). As explained above, the lack of retrieved HCOOH columns in autumn and winter is due to too low thermal contrasts, not exceeding the 5K threshold for the conditional retrievals.

3 Enhancement ratios

Fires emit trace gases in amounts that depend on the specific fire conditions and source material. A useful parameter to quantify trace gas emissions from fires is the emission factor, which is the amount of emitted species per amount of dry fuel (in g kg^{-1}) (Reid et al., 2009). Emission factors are measured both in situ (e.g. Delmas et al., 1995; Yokelson et al., 1999) and in laboratories (Andreae et al., 1988; Koppmann et al., 2005). Large compilations of emission factors, grouped in different source types, can be found
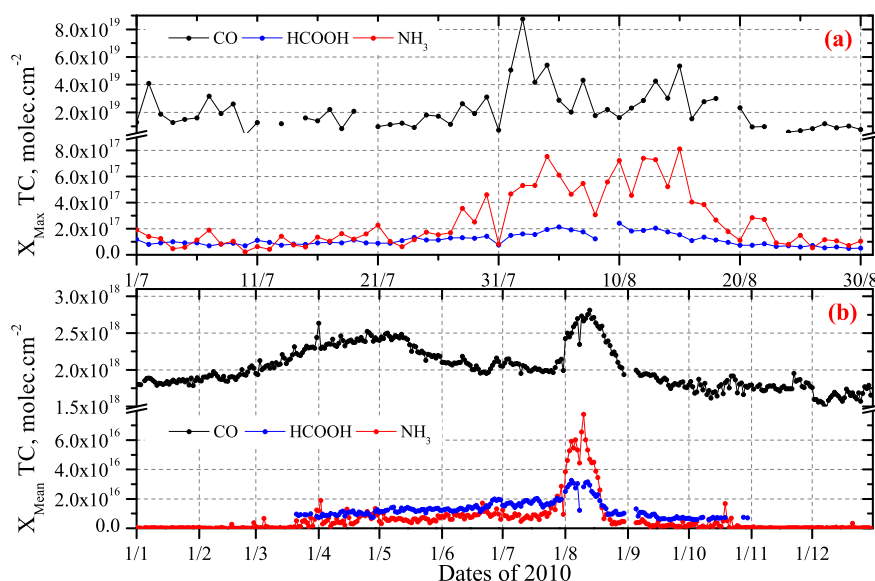
Fig. 2. (a) Temporal evolution of CO (black), NH$_3$ (red) and HCOOH (blue) total column maximums between 1 July and 1 September 2010. **(b)** Mean total column over the area 40–75° N, 30–150° N for CO, NH$_3$ and HCOOH, for the year 2010. Only retrievals with spectral residual root-mean-square less than 3×10^{-7} and 3×10^{-6} W m^{-2} sr^{-1} m for CO and NH$_3$, respectively, were considered here.

in Andreae and Merlet (2001) and Akagi et al. (2011). A related parameter is the emission ratio of a trace gas X, which is the ratio of emitted molecules of X over the number of emitted molecules of a target species such as CO, used hereafter. Emission ratios can be calculated from emission factors by multiplying with the ratio of the molar masses M_{CO}/M_X. In fresh plumes, the emission ratio can be estimated from the ratio of concentrations, the so-called enhancement ratio (Goode et al., 2000):

$$\frac{\Delta X}{\Delta CO} = \frac{[X]_{smoke} - [X]_{ambient}}{[CO]_{smoke} - [CO]_{ambient}}. \tag{1}$$

As the plume ages, the enhancement ratios will typically decrease for species with a lifetime shorter than CO. The time evolution of the enhancement ratio therefore gives insight into the chemical loss processes within the plume (Xiao et al., 2007). When a lot of observations are available, the enhancement ratios can be calculated for each measurement pair ([X],[CO]), while an average enhancement ratio can be estimated from the slope of the linear regression ΔX vs ΔCO (Coheur et al., 2009).

Enhancement ratios for the Russian fires are shown in Fig. 3 over the area defined above. Figure 3a shows an example of the enhancement ratio's calculation. The scatter plots of total columns of NH$_3$ (with RMS (root mean square) less than 3×10^{-6} W m^{-2} sr^{-1} m and HCOOH vs CO on 5 August is presented here. The high correlations (correlation coefficients of 0.75) are indicative of the common emission source for the three species. The series of low NH$_3$ columns ($<10^{16}$ molec cm^{-2}) in Fig. 3a, which are associated with

rather high columns of CO ($>4 \times 10^{18}$ molec cm^{-2}), likely correspond to aged air masses. For this day of 5 August, the calculated enhancement ratios are 0.032 for NH$_3$ and 0.021 for HCOOH. Enhancement ratios are calculated similarly for each day and the corresponding time evolution from 27 July to 24 August is shown in Fig. 3b. Only NH$_3$ total columns with RMS less than 3×10^{-6} W m^{-2} sr^{-1} m are considered here. For NH$_3$ enhancement ratios start around 0.010 on the 27 July and reach a maximum of 0.052 on 10 August when NH$_3$ total columns are largest (Fig. 2b). After that, the enhancement ratio decreases gradually, pointing to a decrease in fire activity and a return to background CO columns. Less pronounced variations of the enhancement ratio are found for HCOOH.

As the 2010 Russian fires are associated with the burning of both peat lands (accounting for 30 % of emitted CO, Konovalov et al., 2011) and other types of vegetation, it is difficult to compare the results to a single emission ratio. We find, however, that for NH$_3$ the range of values measured from IASI (0.010–0.052) is consistent with the values reported in the literature, which average 0.033 for extratropical forest fires, 0.035 for boreal forest fires and 0.097 for peat lands (Akagi et al., 2011).

For HCOOH, the calculated enhancement ratios vary between 0.010 and 0.032 and are much larger than the emission ratios reported in Akagi et al. (2011), which are 2.7×10^{-3}, 2.7×10^{-3} and 1.8×10^{-3} respectively for typical Boreal, extratropical and peat forests fire emissions. The difference between these emission ratios and our calculated enhancement ratios points toward a significant secondary formation
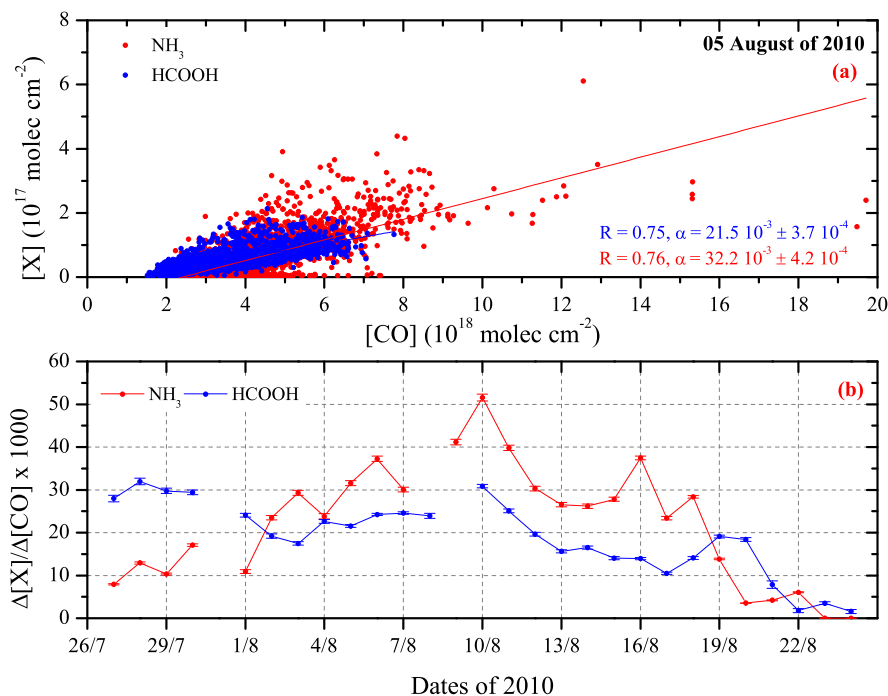
Fig. 3. (a) Scatter plot of NH$_3$ and HCOOH total columns vs CO total columns for 5 August 2010. Linear regressions are plotted for both species as red and blue lines, respectively. The values for the resulting slopes and their errors are given in the figure, along with the correlation coefficient R. **(b)** Temporal evolution of the enhancement ratios of NH$_3$ and HCOOH relative to CO, calculated as the slopes of the linear regressions from 27 July to 24 August, in the region 40–75° N and 30–90° N. The error bars are the corresponding slopes errors.

of HCOOH. Such a secondary production has been reported in a number of studies. Increases in the emission ratios by a factor of 2–2.5 in 2.5 h were found in an Alaskan fire (Goode et al., 2000); a factor of 5.5 in less than a day in a Brazilian fire (Yokelson et al., 2007); a factor of 2.5 in an hour (Yokelson et al., 2009) in Mexico and, finally, by a factor of 7.34 in 4.5 h in a Californian fire (Akagi et al., 2012). The large values found for the enhancement ratios of formic acid are unlikely to be due to an underestimation of the CO total column, which has been shown to be consistent with correlative measurements in various validation studies (e.g. George et al., 2009, Kerzenmacher et al., 2012). As mentioned in Sect. 2, OEM retrievals of formic acid yield columns about a factor of two lower; corresponding enhancement ratios could therefore also be a factor of two lower. The total averaged enhancement ratio found for all the HCOOH OEM retrievals equals 0.011. This is still a factor of five larger than the tabulated emission ratios given by Akagi et al. (2011). Therefore even in this scenario, there is evidence of secondary formation of formic acid and interestingly this 0.011 value is in good agreement with Goode et al. (2000) and Yokelson et al. (2007) who observed enhancement ratios (corrected for spectroscopy – see interactive comment of Yokelson et al., 2013) in downwind plumes from forest fires in the range of ∼ 0.011–0.014. Recent reported values of enhancement ratios from occultation measurements are generally below

0.005, but these observations are made in the upper troposphere and further downwind of the fires (Coheur et al., 2007; Tereszchuk et al., 2011, 2012). More observations and further research is needed to understand the conditions in which secondary formation of HCOOH is important. Also note that a more general interpretation of the enhancement ratios measured by IASI is hampered by the continuous emission, production and complex transport patterns: the buildup of CO during the entire burning period could in particular mean that the real emission ratios are still higher than our reported enhancement ratios.

As a general comment, determination of enhancement ratios from nadir observations is not ideal since there are differences both in the vertical profile of the different species and in the vertical sensitivity of the measurements, which will affect the retrieved enhancement ratios. Uncertainties related to limited sensitivity of the boundary layer only partially cancel each other out.

4 Total mass

Daily observed total masses, TM$_X$, of species X have been calculated here as follows:

$$\text{TM}_X = \frac{M_X C_X S}{N_a}, \tag{2}$$
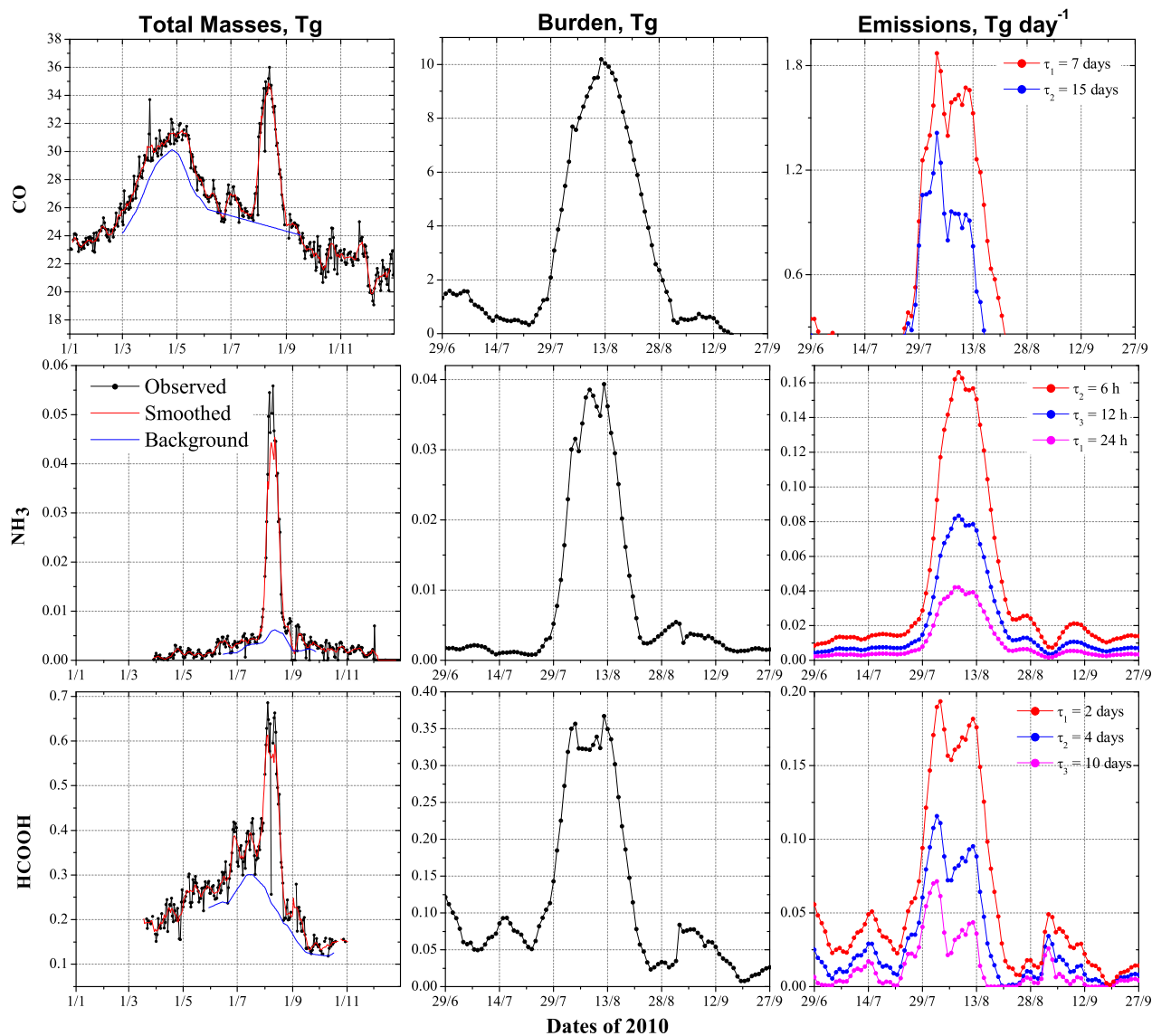
Fig. 4. Left: total CO, NH₃ and HCOOH masses in Tg (black dots and line) over the area 40–75° N, 30–150° N for CO and HCOOH and 40–75° N, 30–90° N for NH₃. The red lines are the smoothed total masses in 10 day intervals; the blue lines are total masses representative of background concentrations. Middle: extra CO, NH₃ and HCOOH smoothed burden in Tg from fires obtained by subtracting background values from the total masses. Right: fluxes in Tg day⁻¹ respectively of NH₃ and HCOOH calculated by Eq. (3).

where M_X is the molar mass of X (in g mol⁻¹), C_X is the mean column retrieved from IASI daytime observations (in molec cm⁻², see Fig. 2b), N_a is the Avogadro number and S represents a defined surface area. For CO and HCOOH the latter corresponds to the red rectangle identified in Fig. 1 and is estimated at 2.75×10^{17} cm². For NH₃, S is a smaller area (40–75° N and 30–90° N) and this is justified by the fact that (Fast Optimal Retrievals on Layers for IASI) FORLI-NH₃ is a conditional retrieval method, as discussed previously, and that the short lifetime of this species prevents its long-range transport. Figure 4 shows, in the left panel, the daily evo-

lution of the total masses for the year 2010 (in black: daily values; in red: smoothed). The total masses reach in mid-August maximums of 36.1 Tg for CO, ∼ 0.06 Tg for NH₃ and 0.70 Tg for HCOOH. The latter should be considered with care, with lower values for HCOOH, considering the possible overestimation of total columns – see Sect. 2.

After having calculated the daily total masses over the area of interest it is possible to estimate the total emissions by making some extra assumptions. Here we follow an approach similar to that of Yurganov et al. (2011). In a first step we estimate the daily total mass due to the fires (the

Table 1. Comparative analysis of total emissions of CO, NH₃ and HCOOH from current and previous studies of the 2010 Russian wildfires.

	CO	NH₃	HCOOH	Comment
Max. daily emission (Tg day⁻¹)				
Fokeeva et al. (2011)	1.2–1.4	–	–	AIRS-MOPITT, standard
Fokeeva et al. (2011)	2.3–2.4	–	–	AIRS-MOPITT, adjusted
Yurganov et al. (2011)	1.5	–	–	IASI-OE, standard
Yurganov et al. (2011)	2.1–2.2	–	–	Estimate from 3 different sounders (IASI, AIRS and MOPITT), adjusted
This study	**1.41–1.87**	**0.04–0.15**	**0.07–0.19**	IASI-OE standard
Total emitted (Tg)				
Fokeeva et al. (2011)	19–26	–	–	AIRS-MOPITT, standard
Fokeeva et al. (2011)	36–42	–	–	AIRS-MOPITT, adjusted
Fokeeva et al. (2011)	12–14	–	–	MODIS, inventory method
Huijnen et al. (2012)	12.2	–	–	MODIS, inventory method (GFASv1.0)
Konovalov et al. (2011)	9.7	–	–	MODIS, inverse modeling
Krol et al. (2012)	20–25	–	–	IASI, inverse modeling
Yurganov et al. (2011)	26.2	–	–	IASI-OE, standard
Yurganov et al. (2011)	34–40	–	–	Estimate from 3 different sounders (IASI, AIRS and MOPITT), adjusted
This study	**19–33**	**0.7–2.6**	**0.9–3.9**	IASI-OE standard

so-called burden) by subtracting total mass background values. The background values (Fig. 4 left panel in blue) were obtained by smoothing the minimum of the total masses observed in 10 day intervals. The resulting burden are plotted in the middle panel in Fig. 4. Maximum burden are calculated at around 10 Tg for CO, 0.04 Tg for NH₃ and 0.37 Tg for HCOOH. A 10 Tg of CO burden represents more than 85 % of total annual anthropogenic emissions in that region (Konovalov et al., 2011) and the NH₃ and HCOOH maximum values reported here account alone for 5 and 20 % of the total annual emissions from extratropical forest fires (Andreae and Merlet, 2001). It should be noted though that for HCOOH the values in Andreae and Merlet (2001) represent primary emissions only.

From the burden we can calculate emission fluxes (in Tg day⁻¹) assuming a simple box model and first order loss terms (Jacob, 1999):

$$E_{i+1}(X) = \frac{B_{i+1} - B_i e^{-t/\tau_{\text{eff}}}}{\tau_{\text{eff}}(1 - e^{-t/\tau_{\text{eff}}})}. \tag{3}$$

Here, E_i and B_i are respectively the flux and the burden on day i, t is time between two observations (here one day) and τ_{eff} is the effective lifetime of the species X. This lifetime term includes chemical losses, but also losses due to transport outside the considered area. Here, we assume that all burden are due to the Russian fires and neglect potential inflow of excess columns. The calculation thus depends exclusively on the effective lifetime, τ_{eff}, of the species. Following estimates of the CO effective lifetime given in Yurganov et al. (2011), the daily fluxes for CO have been estimated using two values of τ_{eff}–namely, 7 and 15 days. As we do not have accurate knowledge of the effective lifetime of HCOOH and NH₃, especially not in such an extraordinary event, we cal-

culate also for these species the fluxes for a range of different lifetimes. This approach allows to conservatively estimate a range of total emissions compatible with the IASI measurements. For HCOOH, we use 2, 4 and 10 days following its global estimated lifetime of 3–4 days (see Stavrakou et al. (2011) and references therein). For NH₃, we use lifetimes of 6, 12 and 24 h as its lifetime ranges typically from a couple of hours to days (Dentener and Crutzen, 1994; Asman et al., 1998; Aneja et al., 2001). The right column in Fig. 4 shows the time evolution of the (smoothed) fluxes in Tg day⁻¹ of these species for these various lifetimes, from 29 June to 27 September 2010. The maximum values calculated this way are 1.41–1.87 Tg day⁻¹, 0.04–0.08–0.16 Tg day⁻¹ and 0.07–0.11–0.19 Tg day⁻¹ for CO, NH₃ and HCOOH respectively, with the larger values logically for the smaller values of τ_{eff}. Finally, total emissions were estimated from these fluxes between 25 July and 31 August 2010 and are 19–33 Tg (CO), 0.7–2.6 Tg (NH₃) and 0.9–3.9 Tg (HCOOH). For NH₃ and HCOOH, this is comparable to what is normally emitted in the course of a whole year by all extratropical forest fires (Galloway et al., 2004; Stavrakou et al., 2011). However for HCOOH, it is important to keep in mind the possible overestimation (by a factor 1.5–2.3) of the BTD retrievals mentioned in Sect. 2.

Several estimates of total emitted CO have been reported in the literature for the 2010 Russian fires, and these have been summarized in Table 1. These include on the one hand estimates derived from CO measurements from the infrared sounders IASI, AIRS (Atmospheric Infrared Sounder) and MOPITT (Measurements of Pollution in the Troposphere) (sometimes coupled with an atmospheric transport model), and on the other hand estimates derived from MODIS (Moderate Resolution Imaging Spectroradiometer) fire radiative

power measurements. In the studies of Yurganov et al. (2011) and Fokeeva et al. (2011), who use direct CO measurements, allowance is made for the limited sensitivity of infrared instruments to boundary layer concentrations by adding an offset estimated from the difference between satellite and ground based measurements, rather than making use of averaging kernels, like is done in the study of Krol et al. (2012) (see below). For these studies the labels "standard" and "adjusted" indicate whether adjustments were made.

There is a large scatter in the data, both for the maximum daily emissions (1.2–2.4 Tg) and the total emitted CO (10–40 Tg). The standard estimates from CO measurements found in Yurganov et al. (2011) (26.2 Tg) and Fokeeva et al. (2011) (19–26 Tg) agree well with our estimates (19–33 Tg). This is not surprising as all three studies use similar approaches. Their adjusted values, with enhanced boundary layer concentrations are about 40 % higher. The total emissions reported here also agree well with the values 20–25 Tg given in Krol et al. (2012) and obtained using inverse modeling of IASI CO data. As they take into account IASI's sensitivity to the boundary layer using averaging kernels this is somehow surprising but points to a possible overcorrection in the papers of Yurganov et al. (2011) and Fokeeva et al. (2011). Differences and potential sources of errors are discussed in detail in Krol et al. (2012). The wide scatter in the data is evidence of the difficulty in estimating total emitted masses from satellite data. For CO our approach gives a rather large but realistic range of values, and gives confidence to our methodology. Likewise, for NH₃ and HCOOH, we have taken several possible effective lifetimes, as to obtain a range of reasonable values for the total emissions.

We can calculate effective emission ratios using the median estimates of the total emissions. Assuming a total CO emission of 26 Tg we obtain for NH₃ an emission ratio of 0.082. This is naturally larger than the observed enhancement ratios 0.010–0.055. For HCOOH an average emission ratio of 0.047 is found, also higher than the observed enhancement ratios (0.020–0.030 for the most active period).

5 Discussion

The sensitivity of IASI to lower tropospheric concentrations of CO, NH₃ and HCOOH depends heavily on the surface–atmospheric temperature difference, the so-called thermal contrast (Clarisse et al., 2010; Razavi et al., 2011). Daytime observations typically have a larger thermal contrast than night-time observations and are the preferred overpass to study these species. FORLI CO retrievals have on average a retrieval error below 10–15 % (Hurtmans et al., 2012). However, the total error can be much larger such as in the case of strong fires (George et al., 2009), especially when there is limited sensitivity to the boundary layer. As we have mentioned in Sect. 4, Yurganov et al. (2011) and Fokeeva et al. (2011) found large underestimates in CO total column

retrievals as compared to ground-based measurements close to Moscow. However, as our total mass estimate is in excellent agreement with a more sophisticated inverse modelling approach of Krol et al. (2012), we do not expect a consistent low bias of the retrieved CO columns.

Retrieval errors for ammonia are larger than for CO, because of smaller signal-to-noise ratios and larger dependence on thermal contrast. Here, NH₃ was conditionally retrieved from IASI spectra, on the basis of a firm spectral signature (which depends on both the total column of NH₃ and the thermal contrast). While we obtain less measurements in this way, the measurements that are retained have limited dependence on the a priori column (low smoothing error). An estimate of the error for NH₃ in the case of extreme conditions as those reported here is outside the scope of this paper, as collocated in situ measurements are the only way to assess it. For agricultural pollution in the boundary layer a retrieval error of 30–50 % for the total column has been estimated (Clarisse et al., 2010). The selection criteria might lead to an underestimate of the total burden and mass of NH₃ (see Sect. 4). Finally, the retrieval of HCOOH relies on conversion from BTDs and is also dependent on the thermal contrast. As in Razavi et al. (2011), we have restricted retrieval to observations with a thermal contrast above 5 K. Razavi et al. (2011) estimate average uncertainties to be about 60 % for such conditions. Independent OEM retrievals performed here indicate a possible overestimation of a factor two.

Systematic errors on the total columns will propagate to the calculation of the enhancement ratios and the emissions. However, random retrieval errors will cancel each other out in the calculation of total masses as this involves integration of many total columns over a large area.

6 Conclusions

The fires that occurred in Russia during the summer 2010 emitted important quantities of trace gases and aerosols for almost a month. In this work, we focused on three trace gases–namely, CO, NH₃ and HCOOH. We presented total columns (maximum and mean) from IASI observations for 2010. We have calculated enhancement ratios of HCOOH and NH₃ relative to CO for each day and reported their time evolution during the fire period. For NH₃, the enhancement ratios were shown to be in good agreement with tabulated values of emission ratios, while for HCOOH our reported values are an order of magnitude larger. Even if we consider an overestimation by a factor of two due to the retrieval method, there is still a difference of a factor of five, supporting evidence of rapid secondary formation of HCOOH in the plumes. For both species the maximum enhancement ratios were found around mid-August, where the total columns are largest. In addition, we have calculated total masses and the burden from fires for each day, as well as fluxes using assumptions on the species lifetimes. For CO, the results

obtained are comparable to previous work. For NH_3 and HCOOH, these are the first values reported. They are of the order of $0.1\,\mathrm{Tg\,day^{-1}}$ depending on the choice of reference lifetime. When integrated over the entire fire period (July–August 2010), the emission fluxes translate to a total emitted mass of 19–33 Tg for CO, 0.7–2.6 Tg for NH_3 and 0.9–3.9 Tg for HCOOH. For all these species, there is a significant contribution to the yearly global emission. For instance, this is for NH_3 and HCOOH comparable to what is emitted in a year by all extratropical forest fires. This study also highlights the difficulty in retrieving HCOOH from nadir observations.

References

Akagi, S. K., Yokelson, R. J., Wiedinmyer, C., Alvarado, M. J., Reid, J. S., Karl, T., Crounse, J. D., and Wennberg, P. O.: Emission factors for open and domestic biomass burning for use in atmospheric models, Atmos. Chem. Phys., 11, 4039-4072, doi:10.5194/acp-11-4039-2011, 2011.

Akagi, S. K., Craven, J. S., Taylor, J. W., McMeeking, G. R., Yokelson, R. J., Burling, I. R., Urbanski, S. P., Wold, C. E., Seinfeld, J. H., Coe, H., Alvarado, M. J., and Weise, D. R.: Evolution of trace gases and particles emitted by a chaparral fire in California, Atmos. Chem. Phys., 12, 1397–1421, doi:10.5194/acp-12-1397-2012, 2012.

Andreae, M. O. and Merlet, P.: Emission of trace gases and aerosols from biomass burning, Global Biogeochem. Cy., 15, 955–966, doi:10.1029/2000GB001382, 2001.

Andreae, M. O., Browell, E. V., Garstang, M., Gregory, G. L., Harriss, R. C., Hill, G. F., Jacob, D. J., Pereira, M. C., Sachse, G. W., Setzer, A. W., Dias, P. L. S., Talbot, R. W., Torres, A. L., and Wofsy, S. C.: Biomass-Burning Emissions and Associated Haze Layers Over Amazonia, J. Geophys. Res., 93, 1509–1527, doi:10.1029/JD093iD02p01509, 1988.

Aneja, V., Bunton, B., Walker, J., and Malik, B.: Measurement and analysis of atmospheric ammonia emissions from anaerobic

lagoons, Atmos. Environ., 35, 1949–1958, doi:10.1016/S1352-2310(00)00547-1, 2001.

Asman, W. A. H., Sutton, M. A., and Schjørring, J. K.: Ammonia: emission, atmospheric transport and deposition, New Phytol., 139, 27–48, doi:10.1046/j.1469-8137.1998.00180.x, 1998.

Chubarova, N., Nezval', Ye., Sviridenkov, I., Smirnov, A., and Slutsker, I.: Smoke aerosol and its radiative effects during extreme fire event over Central Russia in summer 2010, Atmos. Meas. Tech., 5, 557–568, doi:10.5194/amt-5-557-2012, 2012.

Clarisse, L., Clerbaux, C., Dentener, F., Hurtmans, D., and Coheur, P.-F.: Global ammonia distribution derived from infrared satellite observations, Nature Geos., doi:10.1038/NGEO551, 2009.

Clarisse, L., Shephard, M. W., Dentener, F., Hurtmans, D., Cady-Pereira, K., Karagulian, F., Damme, M. V., Clerbaux, C., and Coheur, P.-F.: Satellite monitoring of ammonia: A case study of the San Joaquin Valley, J. Geophys. Res., 115, D13302, doi:10.1029/2009JD013291, 2010.

Clarisse, L., R'Honi, Y., Coheur, P.-F., Hurtmans, D., and Clerbaux, C.: Thermal infrared nadir observations of 24 atmospheric gases, Geophys. Res. L., 38, L10802, doi:10.1029/2011GL047271, 2011.

Clerbaux, C., Boynard, A., Clarisse, L., George, M., Hadji-Lazaro, J., Herbin, H., Hurtmans, D., Pommier, M., Razavi, A., Turquety, S., Wespes, C., and Coheur, P.-F.: Monitoring of atmospheric composition using the thermal infrared IASI/MetOp sounder, Atmos. Chem. Phys., 9, 6041–6054, doi:10.5194/acp-9-6041-2009, 2009.

Coheur, P.-F., Herbin, H., Clerbaux, C., Hurtmans, D., Wespes, C., Carleer, M., Turquety, S., Rinsland, C. P., Remedios, J., Hauglustaine, D., Boone, C. D., and Bernath, P. F.: ACE-FTS observation of a young biomass burning plume: first reported measurements of C_2H_4, C_3H_6O, H_2CO and PAN by infrared occultation from space, Atmos. Chem. Phys., 7, 5437–5446, doi:10.5194/acp-7-5437-2007, 2007.

Coheur, P.-F., Clarisse, L., Turquety, S., Hurtmans, D., and Clerbaux, C.: IASI measurements of reactive trace species in biomass burning plumes, Atmos. Chem. Phys., 9, 5655–5667, doi:10.5194/acp-9-5655-2009, 2009.

Crutzen, P. J. and Andreae, M. O.: Biomass Burning in the Tropics: Impact on Atmospheric Chemistry and Biogeochemical Cycles, Science, 250, 1669–1678, doi:10.1126/science.250.4988.1669, 1990.

Delmas, R., Lacaux, J., and Brocard, D.: Determination of biomass burning emission factors: Methods and results, Environ. Monit. Assess., 38, 181–204, doi:10.1007/BF00546762, 1995.

Dentener, F. J. and Crutzen, P. J.: A three-dimensional model of the global ammonia cycle, J. Atmos. Chem., 19, 331–369, doi:10.1007/BF00694492, 1994.

Elansky, N., Mokhov, I., Belikov, I., Berezina, E., Elokhov, A., Ivanov, V., Pankratova, N., Postylyakov, O., Safronov, A., Skorokhod, A., and Shumsky, R.: Gas composition of the surface air in Moscow during the extreme summer of 2010, Doklady Earth Sciences, 437, 357–362, doi:10.1134/S1028334X11030020, 2011a.

Elansky, N. F., Mokhov, I. I., Belikov, I. B., Berezina, E. V., Elokhov, A. S., Ivanov, V. A., Pankratova, N. V., Postylyakov, O. V., Safronov, A. N., Skorokhod, A. I., and Shumskii, R. A.: Gaseous admixtures in the atmosphere over Moscow during the 2010 summer, Izv. Atmos. Ocean. Phys., 47, 672–681,

doi:10.1134/S000143381106003X, 2011b.

European Commission, Joint Research Centre (JRC)/Netherlands Environmental Assessment Agency (PBL): Emission Database for Global Atmospheric Research (EDGAR), release version 4.2, http://edgar.jrc.ec.europa.eu, 2011.

Fokeeva, E., Safronov, A., Rakitin, V., Yurganov, L., Grechko, E., and Shumskii, R.: Investigation of the 2010 July–August fires impact on carbon monoxide atmospheric pollution in Moscow and its outskirts, estimating of emissions, Izvestiya, Atmos. Ocean. Phys., 47, 682–698, doi:10.1134/S0001433811060041, 2011.

Galloway, J., Dentener, F., Capone, D., Boyer, E., Howarth, R., Seitzinger, S., Asner, G., Clevelands, C., Green, P., Holland, E., Karl, D., Michaels, A., Popter, J., Townsend, A., and Vöosmarty, C.: Nitrogen cycles: Past, present and future, Biogeochemistry, 70, 153–226, doi:10.1007/s10533-004-0370-0, 2004.

George, M., Clerbaux, C., Hurtmans, D., Turquety, S., Coheur, P.-F., Pommier, M., Hadji-Lazaro, J., Edwards, D. P., Worden, H., Luo, M., Rinsland, C., and McMillan, W.: Carbon monoxide distributions from the IASI/METOP mission: evaluation with other space-borne remote sensors, Atmos. Chem. Phys., 9, 8317–8330, doi:10.5194/acp-9-8317-2009, 2009.

Golitsyn, G. S., Gorchakov, G. I., Grechko, E. I., Semoutnikova, E. G., Rakitin, V. S., Fokeeva, E. V., Karpov, A. V., Kurbatov, G. A., Baikova, E. S., and Safrygina, T. P.: Extreme carbon monoxide pollution of the atmospheric boundary layer in Moskow region in the summer of 2010, Doklady Earth Sciences, 441, 1666–1672, doi:10.1134/S1028334X11120014, 2012.

Goode, J. G., Yokelson, R. J., Ward, D. E., Susott, R. A., Babbitt, R. E., Davies, M. A., and Hao, W. M.: Measurements of excess O₃, CO₂, CO, CH₄, C₂H₄, C₂H₂, HCN, NO, NH₃, HCOOH, CH₃COOH, HCHO, and CH₃OH in 1997 Alaskan biomass burning plumes by airborne Fourier transform infrared spectroscopy (AFTIR), J. Geophys. Res.-Atmos., 105, 22147–22166, doi:10.1029/2000JD900287, 2000.

Grutter, M., Glatthor, N., Stiller, G. P., Fischer, H., Grabowski, U., Höpfner, M., Kellmann, S., Linden, A., and von Clarmann, T.: Global distribution and variability of formic acid as observed by MIPAS-ENVISAT, J. Geophys. Res., 115, D10303, doi:10.1029/2009JD012980, 2010.

Huijnen, V., Flemming, J., Kaiser, J. W., Inness, A., Leitão, J., Heil, A., Eskes, H. J., Schultz, M. G., Benedetti, A., Hadji-Lazaro, J., Dufour, G., and Eremenko, M.: Hindcast experiments of tropospheric composition during the summer 2010 fires over western Russia, Atmos. Chem. Phys., 12, 4341–4364, doi:10.5194/acp-12-4341-2012, 2012.

Hurtmans, D., Coheur, P.-F., Wespes, C., Clarisse, L., Scharf, O., Clerbaux, C., Hadji-Lazaro, J., George, M., and Turquety, S.: FORLI radiative transfer and retrieval code for IASI, J. Quant. Spectrosc. Radiat. Transf., 113, 1391–1408, doi:10.1016/j.jqsrt.2012.02.036, 2012.

Jacob, D. J.: Introduction to Atmospheric Chemistry, Princeton University Press, 1999.

Kasischke, E. S., Hewson, J. H., Stocks, B., van der Werd, G., and Randerson, J.: The use of ATSR active fire counts for estimating relative patterns of biomass burning – a study from the boreal forest region, Geophys. Res. L., 30, 1969, doi:10.1029/2003GL017859, 2003.

Kerzenmacher, T., Dils, B., Kumps, N., Blumenstock, T., Clerbaux, C., Coheur, P.-F., Demoulin, P., García, O., George, M., Griffith, D. W. T., Hase, F., Hadji-Lazaro, J., Hurtmans, D., Jones, N., Mahieu, E., Notholt, J., Paton-Walsh, C., Raffalski, U., Ridder, T., Schneider, M., Servais, C., and De Mazière, M.: Validation of IASI FORLI carbon monoxide retrievals using FTIR data from NDACC, Atmos. Meas. Tech., 5, 2751–2761, doi:10.5194/amt-5-2751-2012, 2012.

Konovalov, I. B., Beekmann, M., Kuznetsova, I. N., Yurova, A., and Zvyagintsev, A. M.: Atmospheric impacts of the 2010 Russian wildfires: integrating modelling and measurements of an extreme air pollution episode in the Moscow region, Atmos. Chem. Phys., 11, 10031–10056, doi:10.5194/acp-11-10031-2011, 2011.

Koppmann, R., von Czapiewski, K., and Reid, J. S.: A review of biomass burning emissions, part I: gaseous emissions of carbon monoxide, methane, volatile organic compounds, and nitrogen containing compounds, Atmos. Chem. Phys. Discuss., 5, 10455–10516, doi:10.5194/acpd-5-10455-2005, 2005.

Krol, M., Peters, W., Hooghiemstra, P., George, M., Clerbaux, C., Hurtmans, D., McInerney, D., Sedano, F., Bergamaschi, P., El Hajj, M., Kaiser, J. W., Fisher, D., Yershov, V., and Muller, J.-P.: How much CO was emitted by the 2010 fires around Moscow?, Atmos. Chem. Phys. Discuss., 12, 28705–28731, doi:10.5194/acpd-12-28705-2012, 2012.

Langmann, B., Duncan, B., Textor, C., Trentmann, J., and van der Werf, G. R.: Vegetation fire emissions and their impact on air pollution and climate, Atmos. Environ., 43, 107–116, doi:10.1016/j.atmosenv.2008.09.047, 2009.

Mielonen, T., Portin, H., Komppula, M., Leskinen, A., Tamminen, J., Ialongo, I., Hakkarainen, J., Lehtinen, K., and Arola, A.: Biomass burning aerosols observed in Eastern Finland during the Russian wildfires in summer 2010 – Part 2: Remote sensing, Atmos. Environ., 47, 279–287, doi:10.1016/j.atmosenv.2011.07.016, 2012.

Parrington, M., Palmer, P. I., Henze, D. K., Tarasick, D. W., Hyer, E. J., Owen, R. C., Helmig, D., Clerbaux, C., Bowman, K. W., Deeter, M. N., Barratt, E. M., Coheur, P.-F., Hurtmans, D., Jiang, Z., George, M., and Worden, J. R.: The influence of boreal biomass burning emissions on the distribution of tropospheric ozone over North America and the North Atlantic during 2010, Atmos. Chem. Phys., 12, 2077–2098, doi:10.5194/acp-12-2077-2012, 2012.

Paulot, F., Wunch, D., Crounse, J. D., Toon, G. C., Millet, D. B., DeCarlo, P. F., Vigouroux, C., Deutscher, N. M., González Abad, G., Notholt, J., Warneke, T., Hannigan, J. W., Warneke, C., de Gouw, J. A., Dunlea, E. J., De Mazière, M., Griffith, D. W. T., Bernath, P., Jimenez, J. L., and Wennberg, P. O.: Importance of secondary sources in the atmospheric budgets of formic and acetic acids, Atmos. Chem. Phys., 11, 1989–2013, doi:10.5194/acp-11-1989-2011, 2011.

Razavi, A., Karagulian, F., Clarisse, L., Hurtmans, D., Coheur, P. F., Clerbaux, C., Müller, J. F., and Stavrakou, T.: Global distributions of methanol and formic acid retrieved for the first time from the IASI/MetOp thermal infrared sounder, Atmos. Chem. Phys., 11, 857–872, doi:10.5194/acp-11-857-2011, 2011.

Reid, J., Hyer, E., Prins, E., Westphal, D., Zhang, J., Wang, J., Christopher, S., Curtis, C., Schmidt, C., Eleuterio, D., Richardson, K., and Hoffman, J.: Global Monitoring and Forecasting of Biomass-Burning Smoke: Description of and Lessons From the

Fire Locating and Modeling of Burning Emissions (FLAMBE) Program, IEEE J. Selec. Top. Appl. Earth Obs. Remote Sens., 2, 144–162, doi:10.1109/JSTARS.2009.2027443, 2009.

Shvidenko, A., Shchepashchenko, D., Vaganov, E., Sukhinin, A., Maksyutov, S., McCallum, I., and Lakyda, I.: Impact of wildfire in Russia between 1998–2010 on ecosystems and the global carbon budget, Doklady Earth Sciences, 441, 1678–1682, doi:10.1134/S1028334X11120075, 2011.

Stavrakou, T., Müller, J.-F., Peeters, J., Razavi, A., Clarisse, L., Clerbaux, C., Coheur, P.-F., Hurtmans, D., De Mazière, M., Vigouroux, C., Deutscher, N. M., Griffith, D. T., Jones, N., and Paton-Walsh, C.: Satellite evidence for a large source of formic acid from boreal and tropical forests, Nature Geos., 5, 26–30, doi:10.1038/ngeo1354, 2011.

Tereszchuk, K. A., González Abad, G., Clerbaux, C., Hurtmans, D., Coheur, P.-F., and Bernath, P. F.: ACE-FTS measurements of trace species in the characterization of biomass burning plumes, Atmos. Chem. Phys., 11, 12169–12179, doi:10.5194/acp-11-12169-2011, 2011.

Tereszchuk, K. A., González Abad, G., Clerbaux, C., Hadji-Lazaro, J., Hurtmans, D., Coheur, P.-F., and Bernath, P. F.: ACE-FTS observations of pyrogenic trace species in boreal biomass burning plumes during BORTAS, Atmos. Chem. Phys. Discuss., 12, 31629–31661, doi:10.5194/acpd-12-31629-2012, 2012.

Turquety, S., Hurtmans, D., Hadji-Lazaro, J., Coheur, P.-F., Clerbaux, C., Josset, D., and Tsamalis, C.: Tracking the emission and transport of pollution from wildfires using the IASI CO retrievals: analysis of the summer 2007 Greek fires, Atmos. Chem. Phys., 9, 4897–4913, doi:10.5194/acp-9-4897-2009, 2009.

Witte, J. C., Douglass, A. R., da Silva, A., Torres, O., Levy, R., and Duncan, B. N.: NASA A-Train and Terra observations of the 2010 Russian wildfires, Atmos. Chem. Phys., 11, 9287–9301, doi:10.5194/acp-11-9287-2011, 2011.

Wooster, M. J. and Zhang, Y. H.: Boreal forest fires burn less intensely in Russia than in North America, Geophys. Res. L., 31, L20505, doi:10.1029/2004GL020805, 2004.

Wooster, M. J., Roberts, Perry, G. L. W., and Kaufman, Y. J.: Retrieval of biomass combustion rates and totals from fire radiative power observations: FRP derivation and calibration relationships between biomass consumption and fire radiative energy release, J. Geophys. Res., 110, D24311, doi:10.1029/2005JD006318, 2005.

Xiao, Y., Jacob, D. J., and Turquety, S.: Atmospheric acetylene and its relationship with CO as an indicator of air mass age, J. Geophys. Res., 112, D12305, doi:10.1029/2006JD008268, 2007.

Yokelson, R. J., Goode, J. G., Ward, D. E., Susott, R. A., Babbitt, R. E., Wade, D. D., Bertschi, I., Griffith, D. W. T., and Hao, W. M.: Emissions of formaldehyde, acetic acid, methanol, and other trace gases from biomass fires in North Carolina measured by airborne Fourier transform infrared spectroscopy, J. Geophys. Res., 104, 30109–30125, doi:10.1029/1999JD900817, 1999.

Yokelson, R. J., Urbanski, S. P., Atlas, E. L., Toohey, D. W., Alvarado, E. C., Crounse, J. D., Wennberg, P. O., Fisher, M. E., Wold, C. E., Campos, T. L., Adachi, K., Buseck, P. R., and Hao, W. M.: Emissions from forest fires near Mexico City, Atmos. Chem. Phys., 7, 5569–5584, doi:10.5194/acp-7-5569-2007, 2007.

Yokelson, R. J., Crounse, J. D., DeCarlo, P. F., Karl, T., Urbanski, S., Atlas, E., Campos, T., Shinozuka, Y., Kapustin, V., Clarke, A. D., Weinheimer, A., Knapp, D. J., Montzka, D. D., Holloway, J., Weibring, P., Flocke, F., Zheng, W., Toohey, D., Wennberg, P. O., Wiedinmyer, C., Mauldin, L., Fried, A., Richter, D., Walega, J., Jimenez, J. L., Adachi, K., Buseck, P. R., Hall, S. R., and Shetter, R.: Emissions from biomass burning in the Yucatan, Atmos. Chem. Phys., 9, 5785–5812, doi:10.5194/acp-9-5785-2009, 2009.

Yokelson, R. J., Akagi, S. K., Griffith, D. W. T., and Johnson, T. J.: Interactive comment on "Exceptional emissions of NH$_3$ and HCOOH in the 2010 Russian wildfires" by Y. R'Honi et al., Atmos. Chem. Phys. Discuss., 12, C11864–C11868, 2013.

Yurganov, L. N., Rakitin, V., Dzhola, A., August, T., Fokeeva, E., George, M., Gorchakov, G., Grechko, E., Hannon, S., Karpov, A., Ott, L., Semutnikova, E., Shumsky, R., and Strow, L.: Satellite- and ground-based CO total column observations over 2010 Russian fires: accuracy of top-down estimates based on thermal IR satellite data, Atmos. Chem. Phys., 11, 7925–7942, doi:10.5194/acp-11-7925-2011, 2011.

Zvyaginstev, A. M., Blum, O. B., Glazkova, A. A., kotel'Nikov, S. N., Kuznetsova, I. N., Lapchenko, V. A., Lezina, E. A., Milller, E. A., Milyaev, V. A., Popikov, A. P., Semutnikova, E. G., Tarasova, O. A., and Shalygina, I. Y.: Air pollution over European Russia and Ukraine under the host summer conditions of 2010, Izv. Atmos. Ocean. Phys., 47, 699–707, doi:10.1134/S0001433811060168, 2011.